Air-to-Air Missile Trajectories for Maximization of Launch Range

GERALD M. ANDERSON* AND GEORGE W. WATT†
Air Force Institute of Technology, Wright-Patterson Air Force Base, Ohio

A simplified two-dimensional (horizontal plane) air-to-air missile intercept problem is formulated and analyzed, using the necessary conditions for an optimal trajectory. To achieve the maximum possible launch range against constant-velocity targets, the missile should turn onto a collision course with the target as soon as possible after launch. These maximum launch range trajectories generally include arcs along which the missile uses an intermediate fuel burning rate to maintain a constant velocity. Although this intermediate fuel burning rate is a function of aerodynamic drag, the resulting constant velocity depends only on the effective exhaust velocity of the missile and the component of target velocity in the direction of the final missile velocity vector. The launch range is not very sensitive to errors in this velocity. The optimal time of switching from the maximum fuel burning rate to the intermediate fuel burning rate is completely determined by the target velocity magnitude and direction. These same general features of the optimal fuel-burning-rate program can be expected to appear in more realistic problem formulations.

Introduction

THE ability of an air-to-air missile to fly an intercept trajectory that allows the maximum possible launch range (R_L) is important to both the survivability of the launch aircraft and the attainment of the largest possible launch envelope for the missile. This paper presents the results of an investigation of the missile-turning-rate and fuel-burning-rate characteristics of such trajectories for a simplified air-to-air missile which intercepts a constant-velocity target by maneuvering in a horizontal plane. The mathematical model is presented, then the results of the application of the necessary conditions for an optimal control and for a singular control are given. The solution and results are then discussed.

Mathematical Model for the Intercept Problem

The restriction to a horizontal plane implies that the missile generates just enough vertical lift to offset its weight. Furthermore, the sideslip in the horizontal plane is assumed to be negligible, so that the missile velocity vector is always directed along the missile axis of symmetry. At launch time, $t = 0$, the target is located at the origin of an inertial $X - Y$ coordinate system which is fixed relative to the air, (Fig. 1). The target has a constant velocity V_T directed at an angle θ_T from the X axis. The missile is launched from the position $Y = 0$ and $X = X(0)$ with a velocity V_0 directed at an angle φ_0 from the X axis. The velocity magnitude and direction of the missile are denoted by V and φ, respectively; M is its mass, β is the fuel burning rate, and F is a sideforce control which is used to rotate the missile velocity vector. The state differential equations are

$$\dot{X} = V\cos\varphi, \quad \dot{Y} = V\sin\varphi, \quad \dot{V} = (c\beta - K_d V^2)/M$$
$$\dot{\varphi} = F/MV, \quad \dot{M} = -\beta \tag{1}$$

where $K_d = C_F A\rho/2$, and K_d and the effective exhaust velocity c are assumed to be constant. Induced drag is neglected.

The constraints on the controls β and F are assumed to be independent of V. These constraints are

$$0 \leq \beta \leq \beta_m, \quad -F_m \leq F \leq F_m \tag{2}$$

The boundary conditions are

$$Y(0) = 0, \quad V(0) = V_0, \quad \varphi(0) = \varphi_0, \quad M(0) = M_0$$
$$X(t_f) = V_T t_f \cos\theta_T, \quad Y(t_f) = V_T t_f \sin\theta_T, \quad M(t_f) = M_f \tag{3}$$

where t_f is the unspecified flight time. The quantity to be maximized is the launch range. Since $X(0)$ is negative, this is equivalent to minimizing

$$J = X(0) \tag{4}$$

In analyzing this problem, it is convenient to replace the variable X by the new position variable Z defined by

$$\dot{Z} = -V\cos\varphi, \quad Z(0) = 0 \tag{5}$$

This differential equation and boundary condition replace the X state differential equation and boundary condition in Eqs. (1) and (3), respectively. In terms of Z, the quantity to be minimized is

$$J = V_T t_f \cos\theta_T + Z(t_f) \tag{6}$$

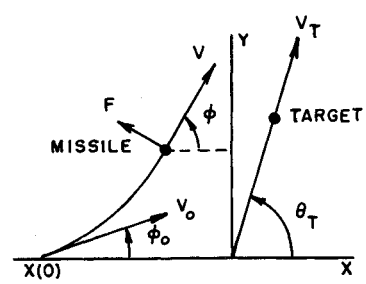

Fig. 1 Geometry of the intercept problem.

Presented as Paper 70-980 at the AIAA Guidance, Control and Flight Mechanics Conference, Santa Barbara, Calif., August 17–19, 1970; submitted August 27, 1970; revision received January 27, 1971.

* Associate Professor, Department of Mechanics. Member AIAA.
† Graduate Student, Department of Mechanics. Member AIAA.

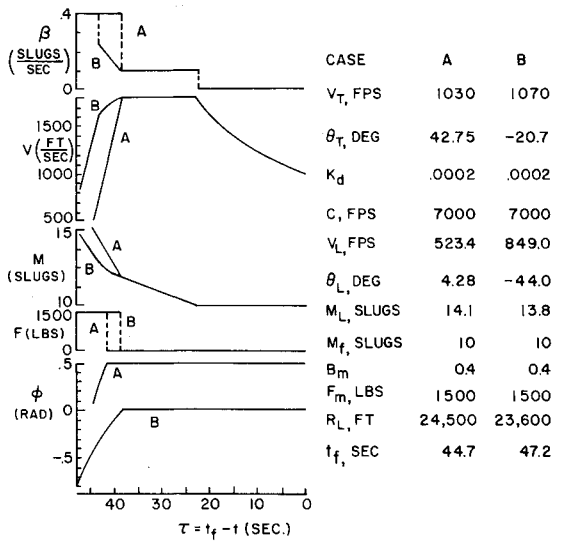

CASE	A	B
V_T, FPS	1030	1070
θ_T, DEG	42.75	-20.7
K_d	.0002	.0002
C, FPS	7000	7000
V_L, FPS	523.4	849.0
θ_L, DEG	4.28	-44.0
M_L, SLUGS	14.1	13.8
M_f, SLUGS	10	10
B_m	0.4	0.4
F_m, LBS	1500	1500
R_L, FT	24,500	23,600
t_f, SEC	44.7	47.2

Fig. 2 Time histories of two maximum-launch-range trajectories.

Application of Necessary Conditions

In this section the necessary conditions for an optimal control[1] and some necessary conditions for a singular control[2,3] are applied to this problem.

Applying the necessary conditions for an optimal control, the Hamiltonian is

$$H = -\lambda_z V\cos\varphi + \lambda_y V\sin\varphi + \lambda_v(c\beta - K_d V^2)/M + \lambda_\phi F/MV - \lambda_m\beta \quad (7)$$

where λ_z, λ_y, λ_v, λ_ϕ and λ_m are costate variables. The costate differential equations are

$$\dot\lambda_z = -\partial H/\partial Z = 0, \quad \dot\lambda_y = -\partial H/\partial Y = 0$$

$$\dot\lambda_v = -\partial H/\partial V = \lambda_z\cos\varphi - \lambda_y\sin\varphi + 2\lambda_v K_d V/M + \lambda_\varphi F/MV^2 \quad (8)$$

$$\dot\lambda_\varphi = -\partial H/\partial\varphi = -\lambda_z V\sin\varphi - \lambda_y V\cos\varphi$$

$$\dot\lambda_m = -\partial H/\partial M = [\lambda_v(c\beta - K_d V^2) + \lambda_\phi F/V]/M^2$$

Transversality conditions give

$$\lambda_v(t_f) = \lambda_\phi = 0, \quad \lambda_z(t_f) = \partial J/\partial Z(t_f) = 1$$
$$H(t_f) = V_T[\lambda_y(t_f)\sin\theta_T - \lambda_z(t_f)\cos\theta_T] \quad (9)$$

where a normal problem has been assumed. Note that the $\dot\lambda_z$ and $\dot\lambda_y$ equations can now be integrated to obtain $\lambda_z(t) = 1$ and $\lambda_y(t)$ is a constant. The controls F and β can be expressed in terms of the switching functions S_F and S_β, which are defined by

$$S_F = \lambda_\varphi/MV, \quad S_\beta = \lambda_v c/M - \lambda_m \quad (10)$$

These controls are given by

$$F = -F_m\,\mathrm{sgn}(S_F), \quad |S_F| \neq 0, \quad F = F_s, S_F = 0; \quad (11)$$

where F_s is a singular control in F, and

$$\beta = \beta_m, \quad S_\beta < 0; \quad \beta = \beta_s, \quad S_\beta = 0;$$
$$\beta = 0, \quad S_\beta > 0 \quad (12)$$

where β_s is a singular control in β.

We next examine the necessary conditions for singular controls in F and β to occur in this problem. There are three situations which must be investigated: $F = F_s$ and $\beta \neq \beta_s$, $F \neq F_s$ and $\beta = \beta_s$, and $F = F_s$ and $\beta = \beta_s$.

First consider the possibility of a singular control in F occurring while $\beta = 0$ or β_m. It is necessary that S_F and all its time derivatives vanish while $F = F_s$. From $S_F = 0$, we find that along a singular arc in F

$$\lambda_\varphi = 0 \quad (13)$$

From $\dot S_F = 0$, we obtain

$$-(\sin\varphi + \lambda_y\cos\varphi) = 0 \quad (14)$$

From $\ddot S_F = 0$, we find that F_s is given by

$$F_s = 0 \quad (15)$$

A further necessary condition is

$$\partial\ddot S_F/\partial F = -(\cos\varphi - \lambda_y\sin\varphi)/M \leq 0 \quad (16)$$

Using Eq. (14), it is easy to show that this condition with pure inequality is satisfied for $-\pi/2 < \varphi < \pi/2$.

For a singular control in β with $F = \pm F_m$, it is necessary that S_β and all its time derivatives vanish. Thus,

$$S_\beta = \lambda_v c/M - \lambda_m = 0 \quad (17)$$

$$\dot S_\beta = (c/M)[\cos\varphi - \lambda_y\sin\varphi + (\lambda_v K_d/M) \times (2 + V^2/c)] + (\lambda_\varphi F/M^2V)(c/V - 1) = 0 \quad (18)$$

where $F = \pm F_m$ in this expression. From Eq. (18) and the expression for $\ddot S_\beta = 0$, the following expression for β_s can be obtained:

$$\beta_s = \{\lambda_v K_d^2 V^2[(V/c)^2 + 4V/c + 2] + (FM/V) \times [(\sin\varphi + \lambda_y\cos\varphi)(2 - V/c) + (K_d\lambda_\varphi/MV) \times (2V + V^2/c + V^3/c^2)]\}/\{K_d\lambda_v c[(V/c)^2 + 4V/c + 2] + (\lambda_\varphi F/V^2)(2 - V/c - 2c/V)\} \quad (19)$$

A further necessary condition is

$$\partial\ddot S_\beta/\partial\beta = K_d\lambda_v c[(V/c)^2 + 4V/c + 2] + (\lambda_\varphi F/V^2)(2 - V/c - 2c/V) \leq 0 \quad (20)$$

This condition must be checked when solving problems with possible singular values of β.

Finally, if $F = F_s$ and $\beta = \beta_s$ occur simultaneously, it is necessary that S_F, S_β and all their time derivatives vanish. For S_F, Eqs. (13–15) are still valid. For S_β, Eqs. (17–19) are valid with $F = 0$ from Eq. (15). Thus, the terms containing F vanish from Eqs. (18) and (19), and Eq. (19) reduces to

$$\beta_s = K_d V^2/c \quad (21)$$

or thrust equals drag on such an arc. A further necessary condition is that the following matrix be positive semidefinite:

$$\begin{bmatrix} -\partial\ddot S_F/\partial F & -\partial\ddot S_F/\partial\beta \\ -\partial\ddot S_\beta/\partial F & -\partial\ddot S_\beta/\partial\beta \end{bmatrix} \quad (22)$$

It is easy to show that $\partial\ddot S_\beta/\partial F = \partial\ddot S_F/\partial\beta = 0$ in this case. Thus, the necessary condition is satisfied if $\partial\ddot S_F/\partial F$ and $\partial\ddot S_\beta/\partial\beta$ are not positive. Equation (16) is valid here so that $\partial S_F/\partial F < 0$ for $-\pi/2 < \varphi < \pi/2$. Equation (20) with $\lambda_\varphi = 0$ gives $\partial\ddot S_\beta/\partial\beta$, which is negative if $\lambda_v < 0$, so that matrix (22) is positive definite if $\lambda_v < 0$ and $-\pi/2 < \varphi < \pi/2$.

The solution to our problem can now be found from the solution of the two-point boundary-value problem given by Eqs. (1, 3, 7–12, 15, and 19), with the X equation of Eqs. (1) and the boundary condition on X replaced by Eqs. (5).

Problem Solution

An analysis of the two-point boundary-value problem shows that the only possible control sequences[1] in F are $\{F_m\}$, $\{-F_m\}$, $\{0\}$, $\{F_m,0\}$ and $\{-F_m,0\}$. Since the first two sequences would be expected to occur only under very restrictive circumstances, they are not considered further.

The possible sequences in β are $\{\beta_m\}$, $\{\beta_m,0\}$, $\{\beta_s,0\}$, $\{\beta_m,\beta_s,0\}$ and $\{0,\beta_s,0\}$, where β_s is given by Eq. (19) if $F = \pm F_m$ and by Eq. (21) if $F = 0$. Since $\{\beta_m\}$ can be expected to occur only under very restrictive boundary conditions on the problem, this sequence is not considered further.

Note from Eq. (14) that if $F(t_f) = 0$, λ_y is given by

$$\lambda_y = -\tan\varphi(t_f) \tag{23}$$

If, in addition, $\beta = 0$ just prior to intercept, Eqs. (7, 9, and 23) can be combined and evaluated at t_f to obtain the following expression for $V(t_f)$:

$$V(t_f) = V_T \cos[\theta_T - \varphi(t_f)] \tag{24}$$

In order to investigate the characteristics of these maximum launch range trajectories, we need solutions for the arcs on which the various possible combinations of F and β occur. In finding these solutions, it is convenient to integrate the two-point boundary-value problem backwards in time from t_f. To do this, we introduce a new time variable $\tau = t_f - t$. Writing the differential equations given by Eqs. (1, 5, and 8) in terms of τ simply changes the sign of the right-hand side of each equation. We next present solutions (closed-form when possible) for arcs on which $F = 0$ and $\beta = 0$, $F = 0$ and $\beta = \beta_s$, $F = 0$ and $\beta = \beta_m$, $F = \pm F_m$ and $\beta = 0$, $F = \pm F_m$ and $\beta = \beta_s$, and $F = \pm F_m$ and $\beta = \beta_m$.

An arc with $F = 0$ and $\beta = 0$ can only be the final arc on a maximum launch range trajectory. During such an arc the solutions for the state variables are

$$\begin{gathered} M = \text{const} = M_f, \quad \varphi = \text{const} = \varphi_f \\ V = V_f/(1 - K_d V_f \tau/M_f) \\ Z = Z_f - (M_f/K_d)\cos\varphi_f \ln(1 - K_d V_f \tau/M_f) \\ Y = Y_f + (M_f/K_d)\sin\varphi_f \ln(1 - K_d V_f \tau/M_f) \end{gathered} \tag{25}$$

where the subscript f refers to the state variables evaluated at t_f.

If an arc with $F = 0$ and $\beta = \beta_s$ precedes the $F = 0$ and $\beta = 0$ arc, the time τ_s of switching in β is completely determined by Eq. (18) with $F = 0$. Using Eqs. (25), the λ_v differential equation can be integrated for the period when $F = 0$ and $\beta = 0$. Substituting the resulting expression for $\lambda_v(\tau)$ into Eq. (18), τ_s can be found to be given by

$$\tau_s = M_f\{(3 + V_f/c) - [1 + 6V_f/c + (V_f/c)^2]^{1/2}\}/(4K_d V_f) \tag{26}$$

During the period when $F = 0$ and $\beta = \beta_s$, the solutions for the state variables and β are

$$\begin{gathered} V = V_s = 4V_f/\{1 - V_f/c + [1 + 6V_f/c + (V_f/c)^2]^{1/2}\} \\ \beta_s = K_d V_s^2/c, \quad \varphi = \varphi_f, \quad M = M_f + \beta_s(\tau - \tau_s) \\ Z = Z_s + V_s(\tau - \tau_s)\cos\varphi_f, \\ Y = Y_s - V_s(\tau - \tau_s)\sin\varphi_f \end{gathered} \tag{27}$$

where the subscript s denotes the conditions at τ_s.

Let the subscript a denote the conditions when switching from $\beta = \beta_m$ to $\beta = \beta_s$ or $\beta = 0$ occurs with $F = 0$. The solutions for M, φ, and V while $F = 0$ and $\beta = \beta_m$ are

$$M = M_a + \beta_m(\tau - \tau_a), \quad \varphi = \varphi_f$$

$$V = Q \times \frac{V_a + Q + (V_a - Q)[1 + (\beta_m/M_a)(\tau - \tau_a)]^{2c/Q}}{V_a + Q - (V_a - Q)[1 + (\beta_m/M_a)(\tau - \tau_a)]^{2c/Q}} \tag{28}$$

where $Q = (c\beta_m/K_d)^{1/2}$. No closed-form solutions could be found for Z and Y on these arcs.

Let the subscript c denote the conditions when switching from $F = \pm F_m$ to $F = 0$ occurs while $\beta = 0$. The solutions for M, V and φ while $F = \pm F_m$ and $\beta = 0$ are

$$\begin{gathered} M = \text{const} = M_c, \quad V = V_c/[1 - K_d V_c(\tau - \tau_c)/M_c] \\ \varphi = \varphi_f \pm (F_m/M_c V_c)[\tau - \tau_c - K_d V_c(\tau^2 - \tau_c^2)/2M_c] \end{gathered} \tag{29}$$

No closed-form solutions could be found for Z and Y during this period.

No closed-form solutions could be found for arcs on which $F = \pm F_m$ and $\beta = \beta_s$ because of the complex dependence of β_s on F, as is shown by Eq. (19). Thus, numerical methods must be used to integrate the differential equations during these arcs.

Let the subscript e denote the conditions when F switches from $F = \pm F_m$ to $F = 0$ while $\beta = \beta_m$. While $F = \pm F_m$ and $\beta = \beta_m$, the solutions for M and V are the same as given in Eqs. (28) with the subscript e replacing a. No closed-form solutions could be found for φ, Z and Y during this period.

Maximum Launch Range Trajectory Characteristics

Figure 2 shows the results for two typical maximum-launch-range trajectories. For case A the trajectory has arcs along which $\beta = \beta_m$ and $F = F_m$, $\beta = \beta_m$ and $F = 0$, $\beta = \beta_s$ and $F = 0$, and $\beta = F = 0$. The trajectory for case B has an arc along which $\beta = \beta_s$ and $F = F_m$ instead of a $\beta = \beta_m$ and $F = 0$ arc. In both trajectories, V_0 is lower than the constant singular velocity V_s which occurs when $\beta = \beta_s$ and $F = 0$. Trajectories with initial arcs of $\beta = 0$ are possible if $V_0 > V_s$. Except for the initial arcs with $\beta = 0$ and $F = \pm F_m$ or 0, these trajectories are similar in character to those shown in Fig. 2.

Note from this figure that the function of the lateral control F is to turn the missile onto a straight-line collision course with the target as soon as possible after launch. Since $\dot{\varphi} = F/MV$, $\dot{\varphi}$ decreases as V increases. In case B, β switches from

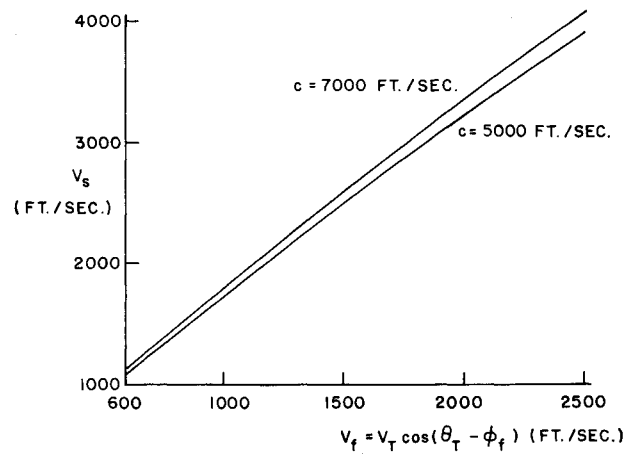

Fig. 3 Singular missile velocity V_s (with $F = 0$) vs final missile velocity V_f for two values of effective exhaust velocities c.

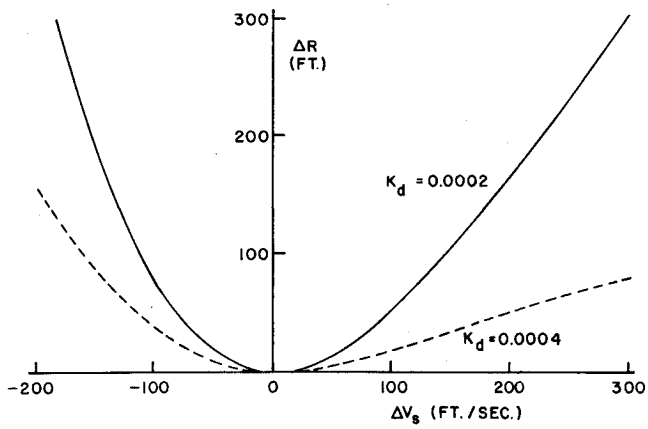

Fig. 4 Reduction in launch range ΔR as a function of the error in the constant singular velocity ΔV_s for two values of K_d for a tail chase problem. For $K_d = 0.0002$, $R_L = 21{,}369$ ft; for $K_d = 0.0004$, $R_L = 10{,}602$ ft (see text for other conditions).

β_m to β_s while $F = F_m$. This switching occurs at a velocity lower than the singular velocity V_s which occurs when $\beta = \beta_s$ and $F = 0$. This early switching to $\beta = \beta_s$ slows the increase in V, so that the collision course is attained earlier than if this switching in β were delayed until $V = V_s$.

The fuel burning rate plays a fundamental role in obtaining the maximum-launch-range trajectory of the missile. Both of the trajectories shown in Fig. 2 have arcs along which $\beta = \beta_s$ and $F = 0$. As can be seen from Eqs. (24) and (27), $V = V_s = \text{const}$ on these arcs and depends only on the effective exhaust velocity c of the missile and V_f, the component of target velocity in the direction of the final missile velocity vector. Figure 3 shows V_s vs V_f for two values of c, and it is seen that V_s increases only slightly as c increases.

Even though V_s is independent of the drag coefficient K_d, the singular fuel burning rate is not, since $\beta_s = K_d V_s^2/c$ along this singular arc. As K_d is increased, more fuel must be expended to overcome drag, thereby reducing the launch range. For $c = 7000$ fps, $\varphi(t) = 0$, $\theta_T = 0$ (i.e., a tail chase), $V_T = 1000$ fps, $V(0) = 1214.7$ fps, $M_0 = 12.674$ slug, and $M_f = 10.0$ slug, the launch ranges are 21,269 ft with $K_d = 0.0002$, and 10,602 ft with $K_d = 0.0004$. On both of these trajectories $V_s = 1795.8$ fps. However, $\beta_s = 0.0921$ slug/sec when $K_d = 0.0002$, and $\beta_s = 0.1843$ slug/sec when $K_d = 0.0004$.

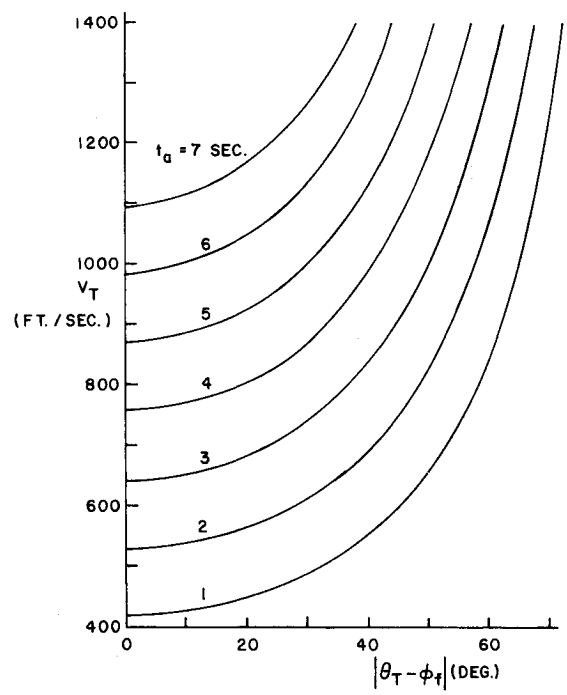

Fig. 5 Curves of constant switching time t_a from $\beta = \beta_m$ to $\beta = \beta_s$ as functions of target velocity magnitude and relative heading for $V_0 = 600$ fps, $M_0 = 14$ slug, $M_f = 10$ slug, $K_d = 0.0002$ and $c = 7000$ fps.

Figure 4 shows the sensitivity of the launch range R_L to errors in V_s for these two tail-chase trajectories. Since R_L is nearly inversely proportional to K_d, ΔR decreases as K_d increases. Negative errors in V_s cause larger reductions in R_L than do positive errors. In any case, R_L does not appear to be very sensitive to small errors in V_s; a 200-fps error decreases it by $<1.5\%$.

In most air-to-air missile trajectories, the missile would normally be expected to be launched on as close to a collision course as possible, and the lateral control force F would be used to produce a small change in φ immediately after launch to get the missile onto an exact collision course. In such problems, arcs with $\beta = \beta_s$ and $F = \pm F_m$ would normally not occur unless the missile were launched at a velocity very close to V_s. Thus, the missile essentially follows a straightline trajectory to intercept the target. The fuel burning rate must be switched from $\beta = \beta_m$ or $\beta = 0$ to $\beta = \beta_s$ at the proper time. This switching time is completely determined by V_T and $|\theta_T - \varphi_f|$. Figure 5 shows curves of constant switching time in the V_T vs $|\theta_T - \varphi_f|$ plane for trajectories with $V(0) = 600$ fps, $M_0 = 14$ slugs, $M_f = 10$ slug, $K_d = 0.0002$ and $c = 7000$ fps. These switching-time curves have the same general form when the parameters of the problem are changed.

Discussion and Conclusions

The simplifying assumptions that were made limit the realism of the problem in that 1) the target will usually be maneuvering rather than be nonmaneuvering, 2) induced drag will reduce R_L if the lateral force control is applied over any significant time period, 3) the missile trajectory will be 3-dimensional, 4) K_d will vary with air density (altitude and temperature) and velocity, and 5) at t_f there should be some negative range rate instead of the ideal zero range rate found in this analysis. Nevertheless, the analysis clearly shows the dependence of R_L on the singular velocity V_s, which occurs when $\beta = \beta_s$ and $F = 0$, and providing for the foregoing items 1–5 probably would not change this general dependence. In particular, if a parabolic drag polar is assumed so that the sideforce F no longer appears linearly in the problem, it is straightforward to show that the necessary conditions for a singular arc in β are still satisfied. However, V_s will no longer be constant, in general.

The formulation of the intercept problem as a differential game would be required to account for maneuvering targets, but it probably would not be meaningful to attempt to maximize R_L. Instead, the problem should be formulated to attempt to find the most efficient fuel burning rate to achieve some goal such as minimizing the miss distance. In Ref. 4 an example is presented of a one-dimensional, pursuit-evasion game in which the dynamics of both the pursuer and the evader are described by equations of the same form as Eqs. (1); the payoff is the final distance between the two vehicles. The fuel burning rates for both vehicles have the same general form as those found in the present analysis. Thus, the formulation of the intercept problem as a differential game does not appear to change the conclusions on the fuel burning rate required to make the optimum use of the available fuel.

It should be further noted that only necessary conditions have been investigated in this problem. The reason for this is that sufficiency conditions for nonlinear problems with both singular and nonsingular arcs have not yet been found. Sufficiency conditions for singular control problems currently exist only for totally singular problems[5–7] and for linear problems with quadratic cost.[8]

References

[1] Athans, M. and Falb, P. L., *Optimal Control: An Introduction to the Theory and Its Applications*, McGraw-Hill, New York, 1966.

[2] Robbins, H. M., "A Generalized Legendre-Clebsch Condition for the Singular Cases of Optimal Control," *IBM Journal of Research and Development*, Vol. 11, No. 4, July 1967, pp. 361–372.

[3] Kelley, H. J., Kopp, R. E., and Moyer, H. G., "Singular Extremals," *Topics in Optimization*, edited by G. Leitmann, Academic Press, New York, 1967, pp. 63–101.

[4] Anderson, G. M., "Necessary Conditions for Singular Solutions in Differential Games with Controls Appearing Linearly," *Proceedings of the First International Conference on the Theory and Application of Differential Games*, Automatic Control Group of the Institute of Electrical and Electronics Engineers, Amherst, Mass., Oct. 1969.

[5] McDanell, J. P. and Powers, W. F., "New Jacobi-Type Necessary and Sufficient Conditions for Singular Optimization Problems," *AIAA Journal*, Vol. 8, No. 8, Aug. 1970, pp. 1416–1420.

[6] Jacobson, D. H. and Speyer, J. L., "Necessary and Sufficient Conditions for Optimality for Singular Control Problems: A Limit Approach," TR-604, March 1970, Div. of Engineering and Applied Physics, Harvard Univ., Cambridge, Mass.; also *Journal of Mathematical Analysis and Applications*, to be published.

[7] Speyer, J. L. and Jacobson, D. H., "Necessary and Sufficient Conditions for Optimality for Singular Control Problems: A Transformation Approach," *Journal of Mathematical Analysis and Applications*, Vol. 33, No. 1, Jan. 1971, pp. 163–187.

[8] Jacobson, D. H., "On Singular Arcs and Surfaces in a Class of Quadratic Minimization Problems," TR 613, Aug. 1970, Div. of Engineering and Applied Physics, Harvard Univ., Cambridge, Mass.; also *Journal of Mathematical Analysis and Applications*, to be published.

JULY 1971 J. SPACECRAFT VOL. 8, NO. 7

A Jupiter Orbiter Mechanics Experiment

CHARLES K. PAUL*
Cornell University, Ithaca, N.Y.

An X-band radar onboard a planetary orbiting spacecraft measuring range and range rate to the planetary surface is not only capable of refining spacecraft orbit determination, but can also be employed to map the planet's gravitational potential. The number of gravitational harmonic coefficients which can be solved is dependent upon the radar accuracy in measuring range rate. In the case of a Jupiter orbiter, spacecraft propulsion penalties and science objectives favor highly eccentric equatorial orbits in which the spacecraft is within radar-measuring range of the planet for only a few hours of the long 40-day period. The radar orbit determination scheme formulated here is thus a short-arc method and the short-term periodic perturbations to the orbit caused by the planet's potential are significant during this close approach phase to the planet. These perturbations on the equatorial orbital elements are derived and expressed as terms of the measured range rate. The theoretical formulation is termed the range rate model and allows solution of four of Jupiter's harmonic coefficients. The only significant nonplanetary perturbations to the measured range rates are caused by Jupiter's closest five natural satellites. The formulation necessary to correct range rates for these perturbations is developed.

Introduction

MAJOR planetary orbiters starting with Jupiter in the early 1980's are logical follow-ups to the late 1970 Grand Tour missions. An orbiter is ideal for studying planetary mass and gravitational properties affecting the spacecraft orbit. The spacecraft utilizes onboard instrumentation provided for other mission objectives, thus no weight or power penalties are associated with this type of experiment.

The theory of satellite geodesy for analyzing the Earth's potential has been well summarized during the past decade.[1] The orbits of geodetic satellites can generally be described as nearly circular with periods of about $1\frac{1}{2}$ hr, the satellite orbiting within one Earth radius of the planet's surface and hence being significantly perturbed by higher order terms of the gravitational potential throughout its orbit. As opposed to terrestrial orbiters, propellant requirements and science objectives dictate highly eccentric orbits about the major planets; e.g., for Jupiter, a 1.1 Jupiter radius (R_J) perijove by 100 R_J apojove orbit is suggested.[2] The orbital period is 45 days and the spacecraft is within $1\frac{1}{2}$ Jupiter radii of the planet's surface for only 2 hr during each orbit. This short duration in the proximity of the planet and the fact that a certain degree of hydrostatic equilibrium suggested by present planetary models of Jupiter[3,4] imply a rapid diminution of the higher order gravity harmonics. Thus only the central term and the second and fourth degree zonals ($J_2 = 0.01470$, $J_4 = -0.00067$)[3,5] of the potential were used to calculate the secular perturbations on various Jupiter orbits.[6] The small secular rates of motion,[6] orbital trim to satisfy science objectives, and secondary perturbational effects during the long duration at apojove caused by other celestial body gravitational fields, solar radiation pressure, propellant tank leakage, and downlink telemetry maneuvers all combine to eliminate the secular and long term orbital rates over an integral number of orbits as a means for zenodetic analysis. Thus direct observation of the short-term periodic effects is predicated. Observation capability implies onboard navigation capabilities in the form of the existing radio transmitter and receiver, the imaging system, and the X-band radar. Deep Space Network (DSN) tracking alone will not suffice when the long $1\frac{1}{2}$ hr radio round trip time, DSN scheduling, and spacecraft perijove occultations from Earth are considered. Figure 1 shows the 1.1 by 100 R_J orbit.

Received September 1, 1970; revision received January 12, 1971. The author wishes to acknowledge the support of NASA under contract NGR 33-010-071 which made possible a large portion of this research.

* Professor of Engineering.